Contact Localization through Spatially Overlapping Piezoresistive Signals

Pedro Piacenza[1,4], Yuchen Xiao[1,4], Steve Park[2,3], Ioannis Kymissis[2] and Matei Ciocarlie[1]

***Abstract*— Achieving high spatial resolution in contact sensing for robotic manipulation often comes at the price of increased complexity in fabrication and integration. One traditional approach is to fabricate a large number of taxels, each delivering an individual, isolated response to a stimulus. In contrast, we propose a method where the sensor simply consists of a continuous volume of piezoresistive elastomer with a number of electrodes embedded inside. We measure piezoresistive effects between all pairs of electrodes in the set, and count on this rich signal set containing the information needed to pinpoint contact location with high accuracy using regression algorithms. In our validation experiments, we demonstrate submillimeter median accuracy in locating contact on a 10mm by 16mm sensor using only four electrodes (creating six unique pairs). In addition to extracting more information from fewer wires, this approach lends itself to simple fabrication methods and makes no assumptions about the underlying geometry, simplifying future integration on robot fingers.**

I. INTRODUCTION

Tactile sensing modalities for robotic manipulation have made great strides over the past years. Recent surveys list numerous such methods: piezoresistance, piezocapacitance, piezoelectricity, optics, ultrasonics, etc. Still, these advances in sensing modalities are only slowly translating to improved abilities for complete robotic manipulators. A possible reason is that the gap between an individual taxel and a touch-sensitive hand often proves difficult to cross. As a recent survey concludes: "Instead of inventing 'yet another touch sensor,' one should aim for the tactile sensing system. While new tactile sensing arrays are designed to be flexible, conformable, and stretchable, very few mention system constraints like [...] embedded electronics, distributed computing, networking, wiring, power consumption, robustness, manufacturability, and maintainability." [1]

In this paper, we focus on the problem of using a touch sensing modality to achieve high-resolution sensing over relatively large areas. Traditionally, this can be achieved using arrays of individual taxels. However, this approach requires at least one wire per taxel, or likely two; thus, an m-by-n taxel array requires $2mn$ wires. At best, matrix addressing can achieve a similar result with $m+n$ wires, but imposes regular geometry on the sensor. Individual taxels must also be isolated from each other, further increasing manufacturing complexity. We are motivated by finding a method to achieve high resolution tactile sensing that circumvents these difficulties and is intrinsically amenable to addressing other system-level aspects from the list above, such as easy manufacturing and coverage of unspecified geometry. In other words, *we are looking for simple ways to achieve high-resolution tactile sensing with few wires*.

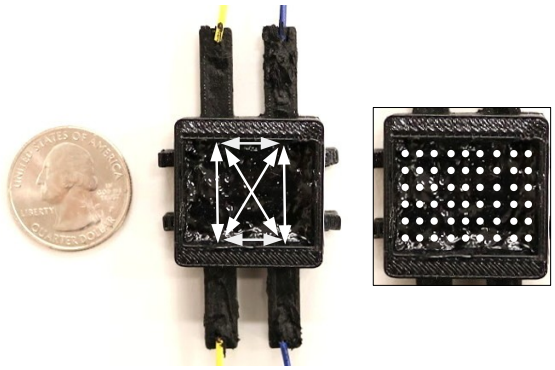

Fig. 1. Proof of concept design, with a rectangular volume of piezoresistive elastomer and four connected electrodes. We measure resistance change due to indentation between all electrode pairs (illustrated by arrows) and use grids of known measurements (illustrated on the right) to learn a mapping from these signals to indentation location.

Our approach, illustrated in Figure 1, is to build a single, continuous volume of a piezoresistive polymer with multiple electrodes embedded in this volume. For an indentation anywhere on the surface of this volume, we measure resistance change in response to strain between all the pairs of electrodes in the area. This provides us with a number of signals that is quadratic in the number of wires. In addition to providing many signals with few wires, this approach has other manufacturability-related advantages: the sensor is a continuous volume that can be poured into a mold of arbitrary geometry. No insulation between various components is necessary.

However, none of these advantages are meaningful if the information carried by the signals from the many pairs of electrodes is not sufficiently discriminative. The price paid for our approach is that the relationship between each signal and the variables of interest is difficult to determine analytically. We thus use purely data-driven techniques and learn this mapping directly from indentation tests. The large number of electrode pairs provides us with a many-to-few mapping to variables of interest, a mapping that can be

[1]Department of Mechanical Engineering, Columbia University, New York, NY 10027, USA.
{pp2511,yx2281,matei.ciocarlie}@columbia.edu
[2]Department of Electrical Engineering, Columbia University, New York, NY 10027, USA.johnkym@ee.columbia.edu,
spark928@alumni.stanford.edu
[3]Department of Materials Science and Engineering, Korea Advanced Institute of Science and Technology, Daejeon, Korea
[4]These authors contributed equally to this work.

effectively learned, as we show in this paper.

Overall, the main contributions of this paper are as follows:

- We introduce a new method for localizing contacts on a touch sensor by measuring resistance changes between multiple, spatially overlapping electrode pairs. This method lends itself to simple fabrication methods well suited for covering non-flat geometry.
- We demonstrate submillimeter median accuracy in determining contact position on a sensor with a 160mm^2 effective area. This is achieved using using only four wires that connect to the sensor, creating six electrode pairs, and without relying on a flat rigid substrate or circuit board.

II. Related Work

Numerous types of transduction principles have been explored during the last two decades when building tactile sensors: resistive, capacitive, optical, ultrasonic, magnetism-based, piezoelectric, tunnel effect sensors, etc. We refer the reader to a number of comprehensive reviews [1], [2] for an overview of these methods. Our goal however is not to explore a new sensing modality; rather, we are looking to build on top of one such method, in order to improve resolution without sacrificing manufacturability.

Our basic building block is an elastomer with dispersed conductive fillers applied to achieve piezoresistive characteristics. Numerous examples of using this method exist in the literature [3], [4], [5], [6], with carbon black and carbon nanotubes as the most commonly employed fillers. Multi-layered designs or additional microstructures can further improve performance [7], [8], [9]. Recently, embedding microchannels of conductive fluids inside an elastic volume [10], [11] has been shown to be an effective alternative to making the entire volume conductive, especially if large strains are desirable. Here however we opt for the simplicity of single volume isotropic materials which can be directly molded into the desired shape.

Regardless of the base transduction principle, attempts to increase spatial resolution have often resulted in the arrangement of multiple discrete sensors into a matrix to cover a given target surface. Some of these arrays can develop very high spatial resolution [12], [13], [14]. However, a drawback of this approach is the difficulty involved in manufacturing these arrays onto a flexible substrate than can conform to complex surfaces. Possible technologies to overcome this problem include organic FETs/thin film transistors realized on elastomeric substrates and other related techniques [15], [16], [17]. Still, wiring and manufacturing complexity, along with other system-level issues such as addressing and signal processing of multiple sensor elements, remain important roadblocks on the way to building complete sensing systems.

Our approach is to maintain the manufacturability and simplicity of single-volume piezoresistive materials, while attempting to harvest a large number of signals from many pairs of electrodes embedded in the volume. We do not aim for analytical characterization of these signals; rather, we aim to directly learn the mapping between this data and our variables of interest. We note that machine learning for manipulation based on tactile data is not new. Ponce Wong et al. [18] learned to discriminate between different types of geometric features based on the signals provided by a previously developed [19] multimodal touch sensor. Current work by Wan et al. [20] relates tactile signal variability and predictability to grasp stability using recently developed MEMS-based sensors [21].

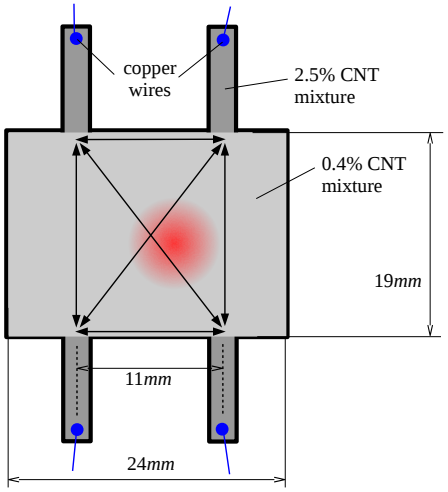

Fig. 2. Design of the proof of concept sensor used for the experiments in this paper. The rectangular center is filled with piezoresistive PDMS/CNT mixture. Side channels are filled with a conductive mixture with higher CNT ratio in order to mechanically isolate copper wire contacts from indentations. For a given indentation (illustrated by red circular pattern) we measure the change in resistance between all six electrode pairs (illustrated by arrows on the surface of the volume).

With traditional tactile arrays, Dang and Allen [22] successfully used an SVM classifier to distinguish stable from unstable grasps in the context of robotic manipulation using a Barrett Hand which provides tactile feedback through four arrays of 24 taxels. Bekiroglu et al. [23] also studied how grasp stability can be assessed based on tactile sensory data using machine-learning techniques like AdaBoost, SVM and HMM with similar success. In similar fashion, both Saal et al. [24] and Tanaka et al. [25] used probabilistic models on tactile data to estimate object dynamics and perform object recognition respectively. However, most of this work is based on tactile arrays built on rigid substrates and thus unable to provide full coverage of complex geometry. In contrast, we apply our methods to the design of the sensor itself, and believe that developing the sensor simultaneously with the learning techniques that make use of the data can bring us closer to achieving complete tactile systems.

III. Sensor Design and Construction

Our overall approach to achieving high spatial resolution starts with a continuous volume of piezoresistive material, with a number of embedded electrodes. Molding a silicone elastomer into the desired shape allows us to embed electrodes while the mixture is viscous, and keeps open the possibility of covering complex, non-flat surfaces in the

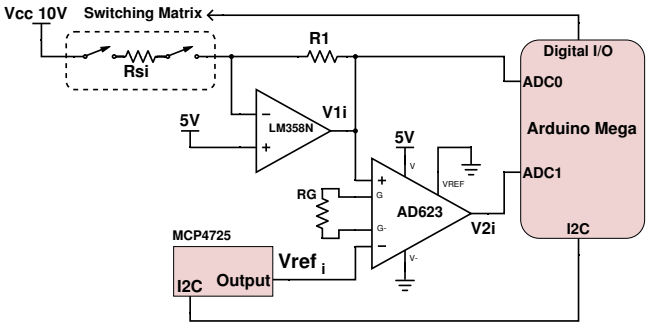

Fig. 3. Measuring circuit. For every terminal pair with a resistance R_{si}, we take a measurement of V_{1i} with the sample at rest. This measured voltage is then reproduced on V_{ref_i} by means of a digital to analogue converter such that we only amplify the change on V_{1i} when the sample is indented.

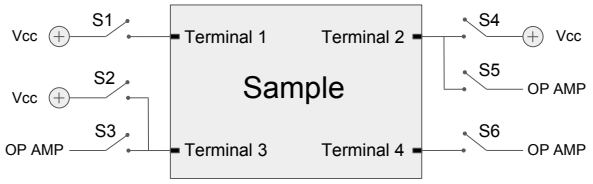

Fig. 4. Switching Matrix structure. All six switches are controlled with digital signals from our microcontroller. This configuration allows us to measure the resistance change across any pair of terminals. The switches must be closed such that we always connect one terminal to Vcc and the remaining one to the inverting input of the operational amplifier.

future. To achieve piezoresistance for our silicone, we use the well established method of dispersing a conductive filler, as detailed below. We then describe the switching circuit developed so that we can sample the change in resistance between any pair of electrodes at high rates.

A. Building a Piezoresistive Material

We disperse multiwall carbon nanotubes (MWCNT, purity: 85%, Nanolab Inc.) into polydimethylsiloxane (PDMS, Sylgard 184, Dow Corning), a two-part silicone elastomer. The key aspect of this process for achieving piezoresistance is choosing the appropriate ratio of conductive filler to elastomer. According to the commonly used percolation theory, the conductivity of the composite w.r.t. filler ratio displays an inflection near a point referred to as the percolation threshold. A composite with that ratio will also display the most pronounced piezoresistive effect [26]. In order to find the percolation threshold of our materials, we built and tested a series of samples with the concentrations of MWCNTs from 0.2wt.% to 5wt.%. We found that the most pronounced change in conductivity occured around the threshold of 0.4wt.% filler, which we used in all subsequent experiments.

In order to achieve uniform distribution of carbon nanotubes within PDMS, we use a chloroform as a common solvent, an approach referred to as the solution casting method [27]. First, we add chloroform and MWCNT into a beaker and sonicate with a horn-type ultrasonicator in a pulse mode with 50% amplitude for 30 min to evenly disperse MWCNTs into chloroform. After that, we pour PDMS into the beaker (at chloroform:PDMS weight ratio of 6:1 or more to reduce the viscosity of the whole mixture), stir the mixture for 5 min to diffuse the PDMS into the solvent, and then sonicate again for 30 min to disperse the MWCNTs into PDMS. We then heat the mixture at 80° C for 24 hours to evaporate the chloroform. After adding the curing agent, the mixture is ready to be poured into the mold; for the experiments presented here we empirically selected a curing agent to PDMS ratio of 1:20. Finally, the sample is finished after curing in an oven at 80° C for 4 hours.

Our goal for this design is to measure resistance through a volume between multiple pairs of terminals. However, in order to isolate piezoresistive effects from mechanical changes at the contacts due to indentation, we mechanically separated the wire contacts from the piezoresistive sample placed under indentation tests. We extended a number of 30mm side channels from the sample, each filled with a CNT-filled PDMS mixture with a higher concentration of 2.5wt.% We then embedded copper wires directly into the mixture at the end of these channels (Figure 2). The mixture with the ratio of 2.5wt.% has no piezoresistive characteristics and its conductivity is close to that of the copper wires; thus, the mixture with the ratio of 0.4wt.% located at the center of the mold dominates the overall conductivity.

B. Sampling Circuit

The main objective for our sampling circuit is to measure the change in resistance between all pairs of electrodes/terminals that occurs as a result of some strain being applied to our sample material. We found that this change can be around 5% of the nominal value at rest. Furthermore, every pair of terminals will have different resistance values at rest. It is also important to be able to sample these relatively small changes in resistance at a high enough rate such that a set of all measurements across terminals can be representative of the instantaneous strain applied.

Consider R_{si} to be the resistance across the i-th terminal pair that we are interested in measuring, $i \in \{1, 2, 3, 4, 5, 6\}$. As shown in Figure 3, we use a first stage with a simple operational amplifier in inverting configuration in a way that we guarantee an output V_{1i} between 0 and 5 volts such that it can be directly measured by our microcontroller analogue to digital converter module (ADC). The output of this stage, V_{1i}, is given by equation 1

$$V_{1i} = 5\text{V} - 5\text{V}\left(\frac{R_1}{R_{si}}\right) \tag{1}$$

Since the change in the resistance R_{si} can be very small, it stands to reason that the change in our output voltage V_{1i} from this first stage will also be small. It is worth noting that the value of R_1 has to be smaller than any of our values R_{si}, and the sensitivity of V_{1i} with respect to R_{si} changing increases as the value of R_1 is closer to those of R_{si}.

Because we are not interested in the absolute value of V_{1i} but only in its change over time when strain is applied, we take a baseline measurement of V_{1i} when the sample is undisturbed. These baseline measurements are then used as

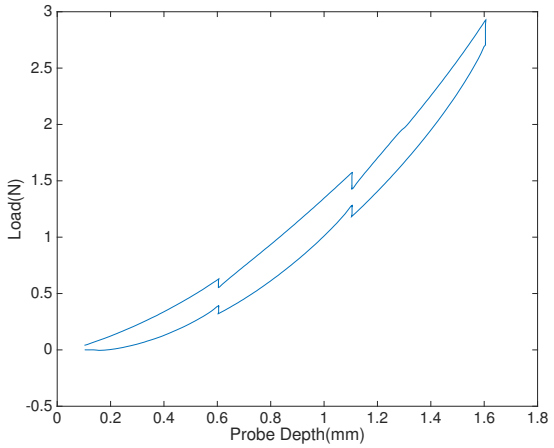

Fig. 5. Load vs. indentation depth for our CNT-filled PDMS samples, in loading and unloading regimes. Measurements were taken by advancing or retracting the probe in steps of 0.5mm separated by 30s pauses.

the values of V_{ref_i} that we hold on the negative input of an instrumentation amplifier for the second stage of the circuit. This allows us to remember the undisturbed value of V_{1i}, compare it with the current one, and amplify that difference. The voltage V_{ref_i} is provided in our circuit by a digital to analogue converter (DAC, MCP4725).

Our switching matrix is shown in Figure 4, where we have six switches total, allowing us to measure across any combination of terminals, T1 through T4. Each one of these terminal pairs has a value of R_{si}, where $i \in \{1, 2, 3, 4, 5, 6\}$. The overall circuit delivers the set of all six V_{2i} values every 25 milliseconds, resulting in a 40Hz sampling frequency. This value is deliberately conservative, since the only bottleneck on how fast we can switch our matrix is down to the speed of the ADC module.

IV. Data Collection Protocol

To collect training and testing data, we indent the sample at a series of known locations and to a known depth. We place the sample on a planar stage (Marzhauser LStep) and indent vertically using a linear probe. We use a hemispherical indenter tip with a 6mm diameter printed in ABS plastic. All indentations are position-controlled relative to the surface of the sample, which we determine manually by lowering the probe until we observe contact. While we do not have a force sensor in our system, we use indentation depth as a proxy for force. Figure 5 shows load vs. indentation depth for our PDMS samples, determined separately using an Instron testing machine.

For indentation locations, we use two patterns. The *grid indentation pattern* consists of a regular 2D grid of indentation locations, spaced 2mm apart along each axis. However, the order in which grid locations were indented was randomized. This is in contrast with the *random indentation pattern*, where the locations of the indentations were sampled randomly over the surface of the sample (not following any pattern).

TABLE I

Prediction accuracy for indentation location

Predictor	Median Err.	Mean Err.	Std. Dev.
Center predictor	5.00 mm	5.13 mm	2.00 mm
Random predictor	6.30 mm	6.70 mm	3.80 mm
Linear regression	1.75 mm	1.75 mm	0.83 mm
Laplacian ridge regression	**0.97 mm**	**1.09 mm**	**0.59 mm**

For each indentation location, we sampled the signal from each pair of electrodes at multiple indentation depths. Each such measurement resulted in a tuple of the form $\Phi_i = (x_i, y_i, d_i, r_i^1, .., r_i^6)$, where x_i and y_i represent the location of the indentation, d_i is the indentation depth, and $r_i^1, .., r_i^6$ (also referred to collectively as $\boldsymbol{r}_i$) represent the change in the six resistance values we measure between depth d_i and depth 0 (the probe on the surface of the sample). These tuples are used for data analysis as described in the next section.

V. Analysis and Results

Our main goal is to learn the mapping from all terminal pairs readings $\boldsymbol{r}_i$ to the indentation location (x, y). To train the predictor, we collected four data sets in regular grid patterns, totaling 216 indentations. For testing, we collected a dataset consisting of 60 indentations in a random pattern. All indentations were performed to a depth of 3mm, or 50% of the total width of the sample. The metric used to quantify the success of this mapping is the magnitude of the error (in mm) between the predicted indentation position and ground truth. In our analysis below, we report this error for individual test points, as well as its mean, median and standard deviation over the complete testing set.

The baseline that we compare our results against includes a "Center Predictor" and a "Random Predictor". The former will always predict the location of the indentation on the center of our sample, and the later will predict a completely random location within the sample surface. The useful area of our sample is 16mm by 10mm; on our test set, the Center Predictor produces a median error of 5mm, while the random predictor, if given a large test set, converges on a median error of above 6mm.

We first attempted Linear Regression as our learning method. The results were significantly better than the baseline, with a median error of under 2mm. Still, visual inspection of the magnitude and direction of the errors revealed a circular bias towards the center that we attempted to compensate for with a different choice of learning algorithm. The second regression algorithm we tested was Ridge Regression with a Laplacian kernel. The Laplacian kernel is a simple variation of the ubiquitous radial basis kernel, which explains its ability to remove the non-linear bias noticed in linear regression results. In this case, we used the first half of the training data for training the predictor, and the second half to calibrate the ridge regression tuning factor λ and the kernel bandwidth σ through grid search.

The numerical results using both of our predictors, as well as the two baseline predictors, are summarized in Table I. These results are aggregated over the complete test set

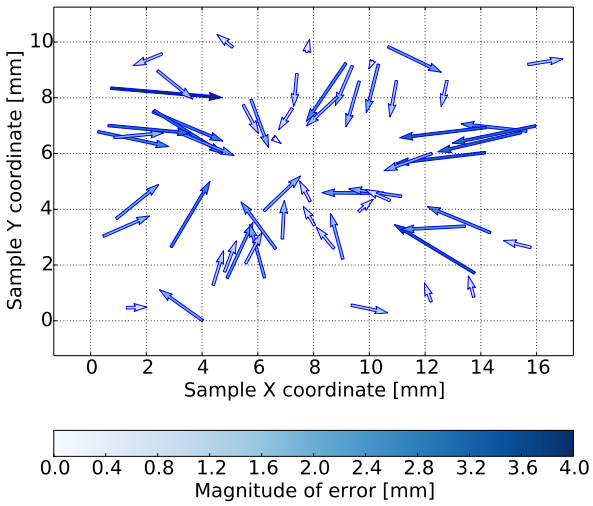

a) Linear regression

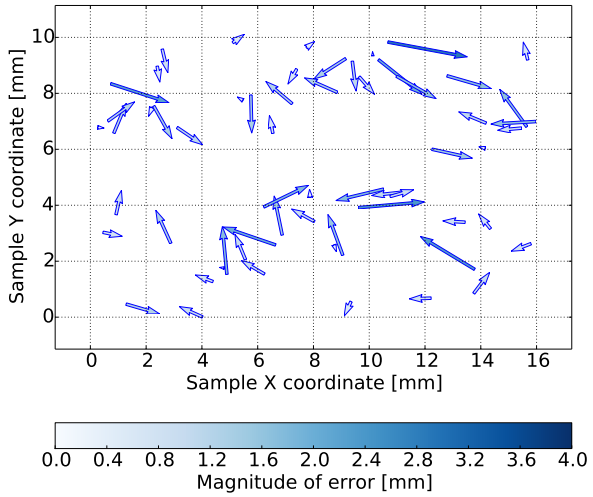

b) Laplacian ridge regression

Fig. 6. Magnitude and direction of localization errors for Linear and Laplacian ridge regressions. Each arrow represents one indentation in our test set; the base of the arrow is at the ground truth indentation location while the tip is at the predicted location.

consisting of 60 indentations. Linear regression identifies the location of the indentation within 2mm on average, while Laplacian ridge regression ($\lambda = 2.7e^{-2}$, $\sigma = 6.15e^{-4}$) further improves this results achieving sub-millimeter median accuracy.

In addition to the aggregate results, Figure 6 illustrates the magnitude and direction of the localization error for the entire test set. To characterize localization error uniformly over the entire sample, we also performed a separate analysis where the test set also consisted of a regular grid of indentations (in this case, we used only three such grids for training and the fourth one for testing). This allows us to plot localization error as a function of position on the surface of the sample; the results are shown in Figure 7. Again the predictor using Laplacian ridge regression achieves high accuracy throughout most of the sample's area, with larger errors occurring on the edges. We believe that this pattern

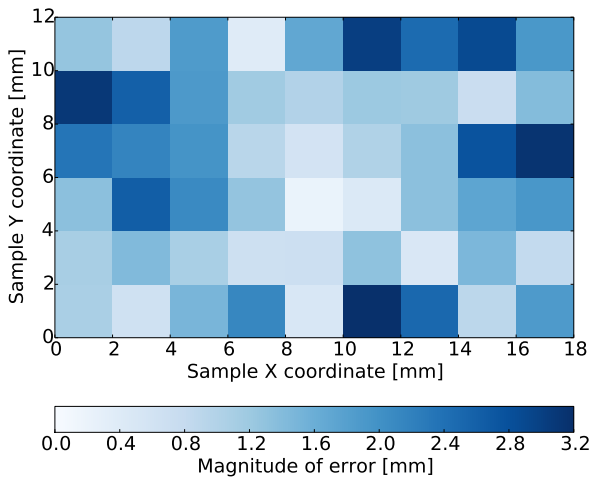

a) Linear regression

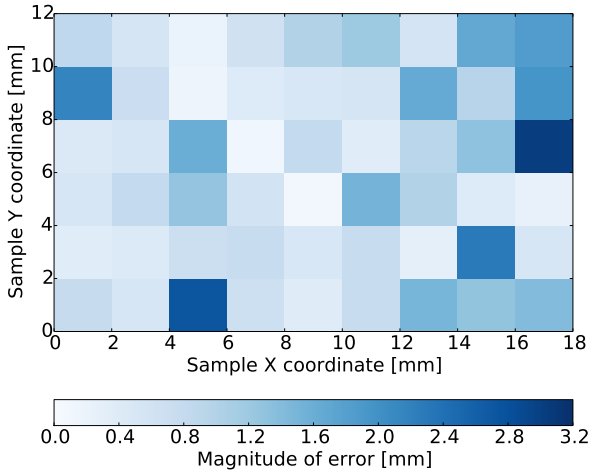

b) Laplacian ridge regression

Fig. 7. Heatmap of localization error magnitude based on indentation location for Linear and Laplacian ridge regression.

can be explained by the fact that an indentation closer to the center is likely to produce a meaningful signal for more electrode pairs compared to an indentation at the edge.

VI. Discussion and Conclusions

Overall, the results support our hypothesis: that we can achieve high accuracy spatial resolution for contact determination over a large sensor area based on a small number of signals collected from spatially overlapping electrode pairs. The proof of concept sensor, built as a rectangular shape with an effective sensing area of 10mm by 16mm, discriminates contact location with submillimeter median accuracy, the equivalent of 160 individual taxels. Even assuming worst-case accuracy throughout the sensor, we can still locate contact within 3mm, the equivalent of 15 taxels. This is achieved by measuring resistance change between 6 electrode pairs, provided by only 4 wires.

Our approach is based on two key ideas. First, the sensor is simply a continuous volume of piezoresistive material; this allows us to measure resistance in response to strain between

any pair of electrodes embedded within. On its upper bound, the number of such pairs is quadratic in the number of wires, and any indentation is likely to excite a multitude of these signals. Second, we do not attempt to model analytically the resulting many-to-many mapping between variables of interest and signals; rather, if such a mapping exists, we believe it can be learned directly from data.

This proof of concept study is meant to illustrate the feasibility of this general approach; as such, there are numerous areas of improvement. Perhaps the most important one will be the ability to also discriminate contact force, or, in our case, indentation depth. Additional variables of interest can include planar shear forces, torsional friction, etc. There are other important aspects that this initial study does not address, such as repeatability, hysteresis, lifespan, sensitivity to environmental factors, etc. We believe that many of these will be determined by the properties of the underlying transducing modality, which has been extensively studied in the literature; however, future work will explicitly investigate these aspects.

Ultimately, the number of variables that can be determined, and the accuracy that they can be determined with, will depend on the raw data that can be harvested from the sensor. In this example, we have demonstrated initial results using 4 electrodes creating 6 unique pairs, but the number of pairs increases fast with the number of electrodes (8 electrodes produce 28 pairs, 12 electrodes yield 66 pairs, etc.). Of course, not all electrode pairs will be sensitive to all indentations, especially if distributed over a large area. Still, these results lead us to believe that it is possible to capture a rich description of the contact using this method. Different methods might also be appropriate for learning the resulting mapping, with new deep learning approaches as prime candidates. We aim to investigate these possibilities in future work.

REFERENCES

[1] R. Dahiya, G. Metta, M. Valle, and G. Sandini, "Tactile sensing: From humans to humanoids," *IEEE Transactions on Robotics*, vol. 26, no. 1, 2010.

[2] M. Hammock, A. Chortos, B. Tee, J. Tok, and Z. Bao, "The evolution of electronic skin (eskin): A brief history, design considerations, and recent progress," *Advanced Materials*, vol. 25, no. 42, 2013.

[3] C. Alex and Z. Bao, "Skin-inspired electronic devices," *Materials Today*, vol. 17, no. 7, 2014.

[4] J. Dusek, M. Triantafyllou, M. Woo, and J. Lang, "Carbon black-pdms composite conformal pressure sensor arrays for near-body flow detection," in *IEEE OCEANS*, 2014.

[5] D. Lipomi, M. Vosgueritchian, B. Tee, S. Hellstrom, J. Lee, C. Fox, and Z. Bao, "Skin-like pressure and strain sensors based on transparent elastic films of carbon nanotubes," *Nature nanotechnology*, vol. 6, no. 12, 2011.

[6] K. Kim, S. Hong, H. Cho, J. Lee, Y. Suh, J. Ham, and S. Ko, "Highly sensitive and stretchable multidimensional strain sensor with prestrained anisotropic metal nanowire percolation networks," *Nano letters*, vol. 15, no. 8, 2015.

[7] S. Mannsfeld, B. Tee, R. Stoltenberg, C. Chen, S. Barman, B. Muir, A. Sokolov, C. Reese, and Z. Bao, "Highly sensitive flexible pressure sensors with micro-structured rubber dielectric layers," *Nature Materials*, vol. 9, pp. 859–864, 2010.

[8] S. Park, H. Kim, M. Vosgueritchian, S. Cheon, H. Kim, J. Koo, T. Kim, S. Lee, G. Schwartz, H. Chang, and Z. Bao, "Stretchable energy-harvesting tactile electronic skin capable of differentiating multiple mechanical stimuli modes," *Advanced Materials*, vol. 26, no. 43, 2014.

[9] X. Wu, S. Suresh, H. Jiang, J. Ulmen, E. Hawkes, D. Christensen, and M. Cutkosky, "Tactile sensing for gecko-inspired adhesion," in *IEEE/RSJ International Conference on Intelligent Robots and Systems*, 2015.

[10] Y. Park, B. Chen, and R. Wood, "Design and fabrication of soft artificial skin using embedded microchannels and liquid conductors," *Sensors*, vol. 12, no. 8, 2012.

[11] D. Vogt, Y. Park, and R. Wood, "Design and characterization of a soft multi-axis force sensor using embedded microfluidic channels," *Sensors*, vol. 13, no. 10, 2013.

[12] B. J. Kane, M. R. Cutkosky, and G. T. A. Kovacs, "A traction stress sensor array for use in high-resolution robotic tactile imaging," *Journal of Microelectromechanical Systems*, vol. 9, no. 4, 2000.

[13] H. Takao, K. Sawada, and M. Ishida, "Monolithic silicon smart tactile image sensor with integrated strain sensor array on pneumatically swollen single-diaphragm structure," *IEEE Transactions on Electron Devices*, vol. 53, no. 5, 2006.

[14] K. Suzuki, K. Najafi, and K. D. Wise, "A 1024-element high-performance silicon tactile imager," *IEEE Transactions on Electron Devices*, vol. 37, no. 8, 1990.

[15] T. Someya, T. Sekitani, S. Iba, Y. Kato, H. Kawaguchi, and T. Sakurai, "A large-area, flexible pressure sensor matrix with organic field-effect transistors for artificial skin applications," *PNAS*, vol. 101, no. 27, 2004.

[16] M. Shimojo, A. Namiki, M. Ishikawa, R. Makino, and K. Mabuchi, "A tactile sensor sheet using pressure conductive rubber with electrical-wires stitched method," *IEEE Sensors Journal*, vol. 4, no. 5, 2004.

[17] D.-H. Kim, J.-H. Ahn, W. M. Choi, H.-S. Kim, T.-H. Kim, J. Song, Y. Y. Huang, Z. Liu, C. Lu, and J. A. Rogers, "Stretchable and foldable silicon integrated circuits," *Science*, vol. 320, no. 5875, pp. 507–511, 2008.

[18] R. D. Ponce Wong, R. B. Hellman, and V. J. Santos, "Haptic exploration of fingertip-sized geometric features using a multimodal tactile sensor," in *Proc SPIE Defense, Security and Sensing / Sensing Technology and Applications Sensors for Next-Generation Robotics Conference*, 2014.

[19] N. Wettels, V. J. Santos, R. S. Johansson, and G. E. Loeb, "Biomimetic tactile sensor array," *Adv Robot*, vol. 22, no. 8, 2008.

[20] Q. Wan, R. P. Adams, and R. Howe, "Variability and predictability in tactile sensing during grasping," in *IEEE International Conference on Robotics and Automation*, 2016.

[21] Y. Tenzer, L. Jentoft, and R. Howe, "The feel of mems barometers: Inexpensive and easily customized tactile array sensors," *IEEE Robotics & Automation Magazine*, vol. 21, no. 3, 2014.

[22] H. Dang and P. K. Allen, "Grasp adjustment on novel objects using tactile experience from similar local geometry," in *Intelligent Robots and Systems (IROS), 2013 IEEE/RSJ International Conference on*, 2013, pp. 4007–4012.

[23] Y. Bekiroglu, J. Laaksonen, J. A. Jorgensen, V. Kyrki, and D. Kragic, "Assessing grasp stability based on learning and haptic data," *IEEE Transactions on Robotics*, vol. 27, no. 3, pp. 616–629, 2011.

[24] H. P. Saal, J. A. Ting, and S. Vijayakumar, "Active estimation of object dynamics parameters with tactile sensors," in *Intelligent Robots and Systems (IROS), 2010 IEEE/RSJ International Conference on*, 2010, pp. 916–921.

[25] D. Tanaka, T. Matsubara, K. Ichien, and K. Sugimoto, "Object manifold learning with action features for active tactile object recognition," in *Intelligent Robots and Systems (IROS 2014), 2014 IEEE/RSJ International Conference on*, 2014, pp. 608–614.

[26] N. Hu, H. Fukunaga, S. Atobe, Y. Liu, and L. J., "Piezoresistive strain sensors made from carbon nanotubes based polymer nanocomposites," *Sensors*, vol. 11, no. 11, 2011.

[27] C. Liu and J. Choi, "Improved dispersion of carbon nanotubes in polymers at high concentrations," *Nanomaterials*, vol. 2, no. 4, 2012.